Title

Comparison of Real-Time Geometric Analyses to Predict Warping Deformation in Fused Filament Fabrication

Authors

Budinoff, Hannah D
Sun, Yilin
McMains, Sara

Publication Date

2020

DOI

10.1115/MSEC2020-8526

Peer reviewed

Proceedings of the ASME 2020 15th International Manufacturing Science and Engineering Conference
MSEC2020
June 22-26, 2020, Cincinnati, OH, USA

MSEC2020-8526

COMPARISON OF REAL-TIME GEOMETRIC ANALYSES TO PREDICT WARPING DEFORMATION IN FUSED FILAMENT FABRICATION

Hannah D. Budinoff[1], Yilin Sun, Sara McMains
University of California, Berkeley
Berkeley, CA

ABSTRACT

This work describes an experimental study to assess if analytical and empirical models can estimate the risk of warping deviation for parts made using fused filament fabrication based on part geometry. We also examine how the accuracy of the prediction varies for different machines and materials. If the predictive models can estimate risk of warping for a given part geometry, they can help enable better design for additive manufacturing so that designers can change part geometry early in the design process to have more easily-manufacturable parts, or choose an alternative orientation to optimize dimensional accuracy at the process planning stage. Specifically, we evaluate the extent to which two analytical models and one empirical model can assess the risk of warping for approximately rectangular parts with varying dimensions. We analyze dimensional accuracy data for parts with different length, height, and fillet type that were printed in ABS and PLA on different fused filament fabrication machines. After evaluating the three models, we found that the empirical model had the best performance over all datapoints. However, the analytical models showed promise but need further refinement on how the prediction of warping deviation depends on part height. Areas for additional research are highlighted.

Keywords: Design for additive manufacturing; fused filament fabrication; warping distortion; dimensional accuracy.

NOMENCLATURE

α	Coefficient of thermal expansion
σ_Y	Yield strength
E	Young's modulus
Δh	Layer thickness
l	Length of part
T_g	Glass transition temperature
T_e	Temperature of build environment

1. INTRODUCTION

Although significant improvements have been made in the past decade, parts manufactured using additive manufacturing (AM) still suffer from unpredictable quality. Efforts have been made to optimize process parameters to improve part quality, but there is still a need for simultaneous efforts to identify risk factors associated with part geometry that lead to dimensional inaccuracy. Warping is one important source of inaccuracy, especially for large fused filament fabrication (FFF) parts. Designers may struggle to make design decisions related to their part geometry early in the design process if they cannot predict the amount of deviation on their printed part. For example, a designer may want to split a large part into two sections to be printed separately, or to choose a particular build orientation of a part with the goal of optimizing dimensional accuracy, but it is currently difficult to make these design decisions without trial prints. Improving design for additive manufacturing (DFAM) education and tool usage in industry has been cited as a major challenge currently facing AM [1]. Predictive models that provide design guidance relating to accuracy and part geometry in near-real-time can help improve DFAM decisions.

There are many different sources of dimensional inaccuracy in parts made using AM. Material properties, environmental conditions, accuracy of the machine used, and build orientation are just some of the factors that can impact dimensional accuracy [2]–[4]. The mechanism that is the focus of this study is warping, also sometimes referred to as curling. Warping is caused by uneven heat distribution during the build process, which causes internal stresses [5]. Distortions caused by warping negatively impact the dimensional accuracy in parts manufactured using several different AM processes [6], but our focus is on FFF, also known as fused deposition modeling.

In FFF, deposited material cools from the extrusion temperature to the temperature of its surrounding environment and shrinks as it cools. Since the material of the first layer

[1] Contact author: hdb@berkeley.edu

adheres to the build platform, however, it cannot shrink freely, and so stresses develop. Additional material is deposited at the extrusion temperature on top of the previously deposited, cooler layer, contributing further to the presence of thermal gradients in the part. When internal stresses caused by thermal gradients are large enough, significant part distortion due to warping develops during printing or when the part is removed. Schmutzler et al. [7] categorized different types of warping, including the curling effect and trapezoid deformation. Here we focus on the curling effect (Fig. 1), which results in the largest part distortions and has been the focus of the most prior study.

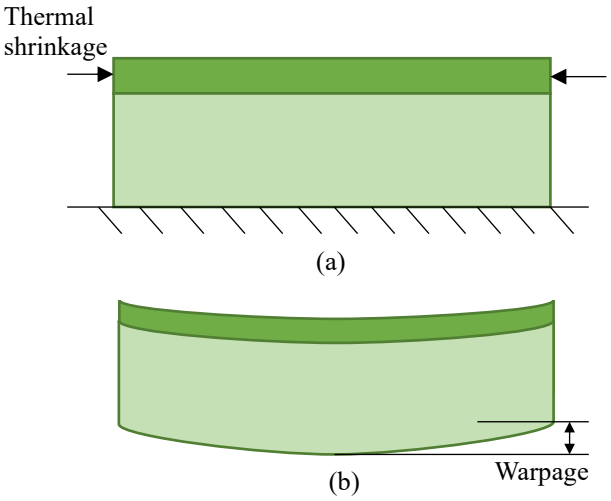

FIGURE 1: (a) THE CURLING EFFECT CAUSED BY THERMAL SHRINKAGE OF EACH NEWLY DEPOSITED LAYER, (b) WHICH TENDS TO CAUSE THE PART TO WARP

The amount of warpage distortion observed is impacted by the part geometry, the thermal properties of the material, and the toolpath chosen [5]. For FFF, polylactic acid (PLA) and Acrylonitrile Butadiene Styrene (ABS) are common material choices. PLA has a lower glass transition temperature (the temperature at which the material transitions from a hard state to a more viscous state, which is slightly lower than the extrusion temperature), which results in less shrinking and warpage than ABS [3]. The temperature of the build platform and the build chamber (or the environmental temperature if no build chamber is present) also impact the amount of observed warpage distortion [5]. Improving adhesion to the build plate by adding an adhesive or heating the build plate to reduce the difference between its temperature and the glass transition temperature can also reduce warping [8].

Modeling efforts for FFF warpage include finite element modeling [9]–[12] and the derivation of analytical models [13]–[15], but the focus of these works is typically on developing recommendations for process parameter settings, not on providing design feedback on part geometry. Some DFAM guidelines do address warping (e.g., a warning that a large area on the build plate will lead to increased warpage [16]), but often do not provide more specific information about geometry risk factors. There is a need for predictive models whose goal is to provide design feedback that is specific and actionable. Models best suited for use in near-real-time for design guidance must maintain a certain level of computational efficiency, often leaving the modeler with a tough choice regarding the balance between the needed level of model complexity and computational efficiency.

Here, we address this problem by exploring the extent to which simple analytical models can be used to provide reliable DFAM feedback regarding warping. We further explore the impact of printer type and part material on model performance. Lastly, we explore the impact of part geometry on observed warpage. Fillets have been cited as a risk factor for excessive warping in several previous experimental studies [17], [18], in design guidelines [19], as well as in online forums for 3D printing, but there is a lack of detailed testing regarding the impact of fillets. Therefore, we performed a series of tests with and without fillets to determine what, if any, impact they had on warping. If filleting corners does impact warping, the analytical models described in the literature would need to be updated to accommodate their influence.

2. MATERIALS AND METHODS

There were three steps to our research. The first step was to print rectangular prism test parts (with and without fillets). Then, the parts were inspected for dimensional and geometric accuracy. Data from a previously published study [13], where a different printer was used, were also included to supplement new data reported here. Finally, the data regarding the parts' geometric accuracy was used to evaluate three different predictive models. Each step is described in detail below.

2.1 Part geometry and printing

A full factorial design of experiments with two levels was used to determine the parts to be printed. We varied the length, height, and the presence of fillets. We did not use width as a control variable because we needed to limit the scope of our experimentation and because previous studies determined the longest dimension of the part, which we refer to here as the length, had the most impact on the measured warping distortion [13]. The width was fixed at 40 mm. The levels of the control factors are shown in Table 1. An example of the printed parts, which are all various sizes of rectangular prisms, is shown in Fig. 2. Eight rectangular prisms were printed on a LulzBot TAZ 5 (an FFF printer manufactured by Aleph Objects, Inc, Loveland, CO) using PLA and a layer thickness of 0.2 mm. The chamber temperature is not controlled on the TAZ 5. Each part was printed in the center of the build platform, by itself. Each part was printed under similar conditions. The time between printing, removal from the build plate, and inspection was similar between parts.

TABLE 1: CONTROL FACTORS AND THEIR LEVELS

Length (mm)	Height (mm)	Filleted corners?
140, 170	3.5, 15	Yes (radius of 5mm), No

To evaluate model performance, we also include data here from Armillotta et al. [13]. The parts they printed were also rectangular prisms, with lengths of 140, 100, or 60 mm, widths of 20 or 60 mm, and height of 1.5, 3.5, or 5.5 mm; they were printed on a Dimension Elite manufactured by Stratasys (Eden Prairie, MN) using a layer thickness of 0.254 mm and ABS filament. The chamber temperature was 75°C. All of the prisms printed by Armillotta et al. [13] were printed without fillets. We use data here from 36 separate prints: 8 which we printed and 24 from the data published by Armillotta.

2.2 Part inspection

The part inspection process for the eight parts we printed had two main components. First, each part was measured for deviations in height using calipers. Then, each part was scanned using a 3D scanner (described in detail below) and inspected for flatness. All measurements focused on quantifying the warpage deviation, but in different manners.

To quantify deviations in height, each part was measured at the same eight points: the four corners and the middle of each side. The first measurement was at the corner where the printing contour started and ended, on the bottom face of the part (Location 1), and then the measurements continued around the part. The measurement locations are shown graphically in Fig. 2. We used a Vernier caliper to measure the height, *h*, of the part at these eight locations. To obtain more accurate measurements, three measurements were taken and averaged at each location. The average of these three measurements was subtracted from the nominal height to obtain a height deviation at each location.

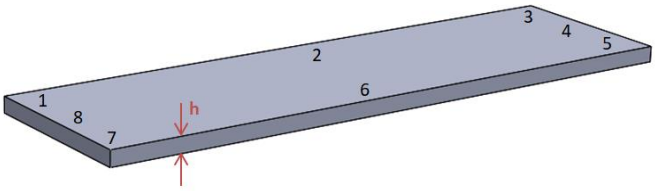

FIGURE 2: DEVIATION IN THE HEIGHT OF THE PART WAS MEASURED AT EIGHT POINTS AROUND THE PART PERIMETER.

The parts were scanned using a ROMER Absolute Arm 7525 SEI produced by Hexagon Manufacturing Intelligence, which has a minimum point spacing of 0.014mm and a theoretical scanning accuracy of 0.063 mm [20]. During the scanning process, we positioned the part on a supporting rod held by a bench vise. This setup allowed the maximum amount of the surfaces to be scanned at once. Each part was scanned twice (once scan of the top and one scan of the bottom) to prevent the supporting rod impacting the scan. After scanning the part, the scan was processed in PolyWorks Inspector, metrology software produced by InnovMetric Software (Québec, Canada). We imported the original CAD model of the part into PolyWorks and compared the nominal CAD with the scan of the printed part to quantify deviations. In PolyWorks, the deviation from nominal at all points was plotted as color maps over the CAD data so that the geometric deviation can be perceived visually. We also used PolyWorks to inspect the parts for the geometric tolerance of flatness on all six sides. Because the measurement of the flatness error on the bottom face of the part corresponded to the deviation predictions of the predictive models that we seek to test, we will focus that measurement. We will refer to the flatness measurement on the bottom face as the flatness error. We also used the scanned data to estimate the relative deviation at each corner, which was measured as the difference between the maximum deviation at each corner and the deviation at the center of the part.

2.3 Description of predictive models

We sought to determine the suitability of different analytical models to predict warping. For this study, two analytical models and an empirical model were assessed: Model 1, which was derived in Wang et al. [14]; Model 2, which is an extension of Model 1 developed by Armillotta et al. [13]; and Model 3, which we present here. We briefly summarize each model here but the reader is referred to the respective sources of the model for more detail on Models 1 and 2.

Model 1 is a prediction of inter-layer warping in FFF parts. As described in [14], the warpage deviation corresponding to flatness of the final part, δ, is calculated as:

$$\delta = \frac{n^3 \Delta h}{6\alpha(T_g - T_e)(n-1)} \left\{ 1 - \cos\left[\frac{3\alpha l}{n\Delta h} (T_g - T_e) \frac{n-1}{n^2} \right] \right\} \quad (1)$$

where n is the number of layers that have been deposited, Δh is the layer thickness, α is the coefficient of thermal expansion, T_g is the glass transition temperature, T_e is the environmental or build chamber temperature, and l length of the part.

Model 2 is based on Model 1 but also includes the impact of plastic deformation during the build process and factors in multi-layer shrinkage. The deviation is predicted to be a function of many of the same variables as the prior equation, with the addition of E, Young's modulus, T_m, the melting temperature, and σ_Y, the yield strength:

$$\delta = \frac{3}{4}\alpha\left(T_g - T_e\right)\frac{l^2 m\Delta h}{h^2}\left(1 - \frac{m\Delta h}{h}\right) \cdot f(h, \Delta h, m, a) \quad (2)$$

where

$$f(h, \Delta h, m, a) = \begin{cases} 1 & \text{if } a \geq \frac{3}{4} \\ 1 & \text{if } a < \frac{4}{3}, h \geq \frac{3m\Delta h}{2 - \sqrt{4 - 3a}} \\ 1 - \frac{1}{4}(2 + c)(1 - c)^2, & \text{if } a < \frac{4}{3}, h < \frac{3m\Delta h}{2 - \sqrt{4 - 3a}} \end{cases}$$

and

$$a = \frac{\sigma_Y}{E\alpha(T_g - T_e)}, b = \frac{m\Delta h}{h}, c = \frac{a-b}{3b(1-b)}$$
$$m \approx 0.5\frac{T_m - T_e}{T_g - T_e}$$

Model 3 is the simplest of the models that we tested. It is based on prior experimental work that showed that the length of the part (measured as the longest dimension of the rectangular part) was the most influential geometric variable affecting the amount of warping of thin, rectangular parts [13]. Model 3 simply states that the warping deviation is proportional to the length of the part, with an experimentally determined constant of proportionality, *k*:

$$\delta = kl \quad (3)$$

In our implementation of the models, we used the following values, referencing ABS properties at elevated temperatures from previous studies on warping [11], [13]. For PLA, we referenced additional references for room temperature properties [21], [22] and assumed that the impact of elevated temperatures on the properties of PLA was similar to the impact seen for ABS. The parameter *k* was determined by choosing one part for a particular material and printer type at random and dividing its measured flatness error by its length. The model parameters we used are summarized in Table 2.

TABLE 2: MODEL PARAMETERS USED TO COMPARE PREDICTIONS TO LULZBOT AND DIMENSION DATA

	LulzBot (PLA)	**Dimension (ABS)**
α [K^{-1}]	$80 \cdot 10^{-6}$	$60 \cdot 10^{-6}$
E [MPa]	2700	1500
σ_Y [MPa]	2.5	1.5
T_m [°C]	170	270
T_e [°C]	30	75
T_g [°C]	60	105
k	$3.34 \cdot 10^{-3}$	$7.67 \cdot 10^{-3}$

3. RESULTS AND DISCUSSION

We divide the results and discussion into two subsections. The first subsection discusses the impact of different geometry factors on the amount of observed warpage deviation. The second subsection evaluates the accuracy of the models' predictions for warpage deviation.

3.1 Impact of geometry on warping

Armillotta et al. [13] found part length and height had significant individual and interaction effects on warpage deviation, while part width did not have a statistically significant individual effect. For the geometry tested in their study [13], the warpage deviation was most strongly influenced by the length of the part.

We printed parts on the LulzBot to further explore the impact of geometry factors on warpage deviation. A three-way analysis of variance (ANOVA) was completed to assess the relative impact of fillets, length, and height on the amount of warpage observed (as measured by largest deviation at each corner relative to the center deviation) on the parts printed on the LulzBot. To ensure that the assumptions of the ANOVA test were met, we conducted several tests. A Lilliefors goodness-of-fit was conducted for each group. This test indicated that the assumption of normality was met. To ensure the assumption of homogeneity of variance was met across the groups, a Levene's test was conducted for the data, which indicated that the assumption of homogeneity. Significant interaction effects were found when two-way interactions were included in the ANOVA**.** The results of this ANOVA are shown in Table 3.

TABLE 3: ANALYSIS OF VARIANCE EVALUATING RELATIVE IMPACT OF DIFFERENT GEOMETRY FACTORS ON RELATIVE CORNER DEVIATIONS

Source	**DOFs**	**SS**	**F**	***p*-value**
Length	1	0.15471	21.3	<.001
Fillets	1	0.02971	4.09	.054
Height	1	1.09705	151.04	<.001
Length*Fillets	1	0.00705	0.97	.3339
Length*Height	1	0.12814	17.64	<.001
Fillets*Height	1	0.03955	5.45	.028
Error	25	0.18158		
Total	31	1.63779		

Part height was found to be a statistically significant main effect. Although some warping was visible on thick parts in our study, the warping was less in magnitude than on thin parts with the same geometry. At 15 mm, the height of the thicker parts was three times larger than the thickest part tested by Armillotta et al., which may be the reason we identified a stronger effect from increasing height than Armillotta et al. did. Length also appeared to be related to an increase in warpage, though its effect was less than that of height. The range of part lengths printed on the LulzBot, from 140 to 170 mm, was also less than previously tested, so this may be the cause of the reduced impact of length compared with what Armillotta et al. observed. Fillets were not found to have a statistically significant effect on the amount of warpage on the bottom face. A statistically significant interaction effects from length and height was observed. From our data, it appears that the effect of length on warpage is most impactful for thin parts, and less impactful for thicker parts. The main effects are shown graphically in Fig. 3, and the interaction plot is shown in Fig. 4.

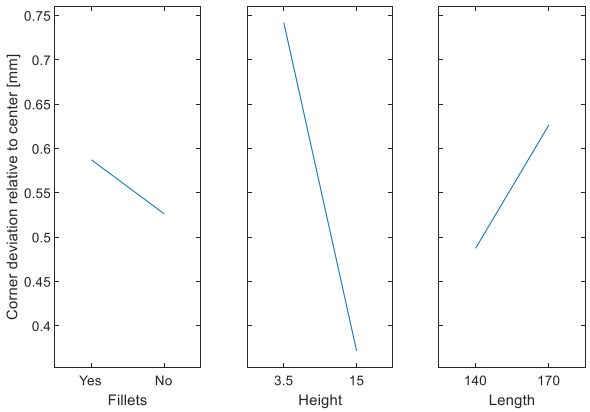

FIGURE 3: MAIN EFFECTS PLOT FOR THE FIRST ANOVA FOR CORNER DEVIATION RELATIVE TO CENTER DEVIATION

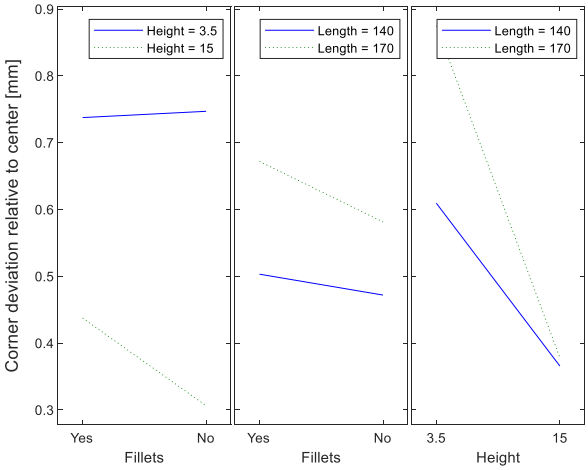

FIGURE 4: INTERACTION PLOT FOR THE FIRST ANOVA FOR CORNER DEVIATION RELATIVE TO CENTER DEVIATION

In addition, fillets were not found to influence the general shape of the warpage deviation on the parts. Table 4 shows the deviation from nominal geometry of the as-printed rectangular prisms. Both filleted and non-filleted parts show upward curling of the outside edges relative to the center. The center of the distortion on both parts is offset from the geometric center of the part, similar to the results seen by Zhang and Chou [9] and Xinhua et al. [23]. In order to enable easy comparison between deviation plots, we restricted the plotted deviations to a range of -0.5 mm to 0.5 mm to create the images shown in Table 4. Data outside of this range appears as a light grey color, as seen in the scans for the thin parts with a length of 140 mm.

TABLE 4: SCANS OF BOTTOM OF PARTS (COLOR SHOWS DEVIATION FROM NOMINAL GEOMETRY IN MM) AND PHOTOS OF PARTS (IN ORIENTATION USED IN PRINTING)

PolyWorks Scans	Photos
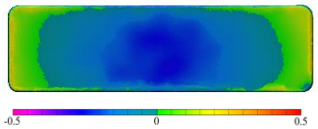	
l = 140mm, h = 15 mm, fillets	
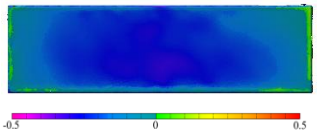	
l = 140mm, h = 15 mm, no fillet	
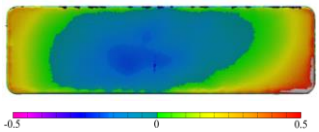	
l = 140mm, h = 3.5 mm, fillets	
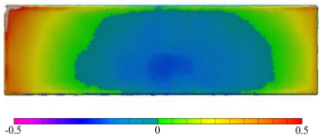	
l = 140mm, h = 3.5 mm, no fillet	
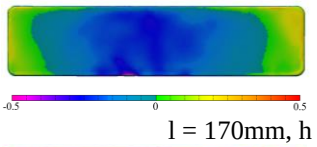	
l = 170mm, h = 15 mm, fillets	
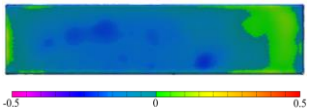	
l = 170mm, h = 15 mm, no fillet	
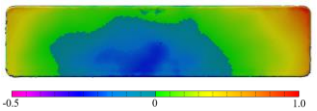	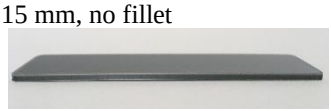
l = 170mm, h = 3.5 mm, fillets	
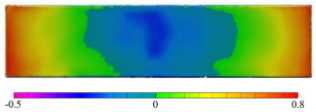	
l = 170mm, h = 3.5 mm, no fillet	

The patterns of deviations in height, as measured with a Vernier caliper, along the edges of the part were similar for parts with and without fillets. The plots of the height deviations around the perimeter of the parts are shown in Fig. 5. For the diagram of point numbering, see Fig. 2. Generally, the parts tended to be slightly undersized, with mostly negative height deviations. The thinner parts seemed to have larger deviations, in general. Fillets seemed to reduce height deviations at the corners for the thinner parts, but this reduction was less obvious for the thicker parts.

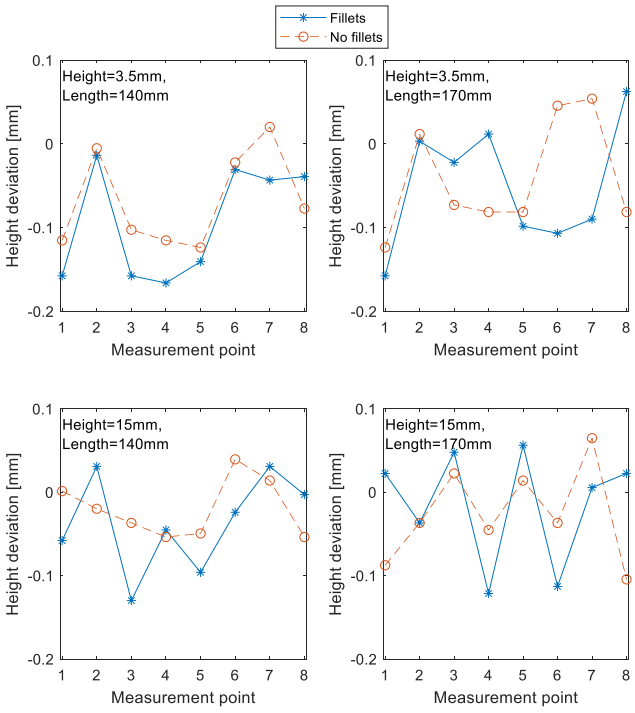

FIGURE 5: HEIGHT DEVIATIONS TENDED TO BE NEGATIVE AND LARGER AT CORNER POINTS (MEAUSUREMENT POINTS 1, 3, 5, AND 7). FILLETS REDUCED DEVIATIONS AT CORNERS FOR THINNER PARTS.

To quantify the relative impacts fillets and the other different geometry factors had on the height deviations, we performed another ANOVA. A Lilliefors goodness-of-fit was conducted for each group, which indicated that the assumption of normality was met for each group. A Levene's test was also conducted, which indicated that the assumption of homogeneity of variance was also met. The results of the ANOVA indicated that no significant interaction effects were found when two-way interactions were included for the height deviation measurements, and so the ANOVA was re-run to exclude these interactions. The results of this second ANOVA are shown in Table 5.

TABLE 5: ANALYSIS OF VARIANCE EVALUATING RELATIVE IMPACT OF DIFFERENT DIMENSIONS AND GEOMETRY ON HEIGHT DEVIATIONS AT CORNERS

Source	DOFs	SS	F	*p*-value
Length	1	0.0021	1.27	.27
Fillets	1	0.0034	2.1	.16
Height	1	0.0212	13.08	.001
Error	28	0.0454		
Total	31	0.0720		

The only statistically significant main effect was associated with height: parts with a height of 15 mm had less height deviations on average than the parts with a height of 3.5 mm. Fillets did seem associated with a decrease in the height deviations, but the effect was not statistically significant (p=.16), possibly due to our relatively small sample size. These effects are shown graphically in Fig. 6.

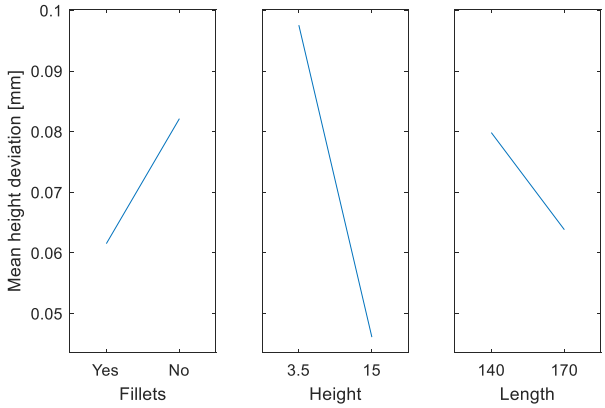

FIGURE 6: MAIN EFFECTS PLOT FOR THE SECOND ANOVA FOR HEIGHT DEVIATION

In general, we found that thick parts tended to warp less than thin parts, as measured by the height deviations and the largest deviation at each corner relative to the center deviation. We did not find a significant effect of length on warping, but this is likely due in part to the small range of lengths that we tested. For parts with fillets, corners appeared to be slightly less deformed when measured as a height deviation. The impact of fillets on the largest deviation at each corner relative to the center deviation was less clear. We hypothesize that at sharp corners on the parts without fillets, internal stresses were large enough that the corners of the part separated from the build plate during printing. This separation could have reduced the internal stresses in the part, which reduced the overall warping of the part slightly, but resulted in larger height deviations. From our preliminary study, it appears that filleted corners may improve adhesion but do not directly impact the curl effect.

3.2 Evaluation of model performance

To evaluate the performance of each predictive model, we calculated root-mean-square error (RMSE) for each model based on the difference between the model predictions and experimental flatness measurements. The RMSE for Model 1 was 0.784 mm, the RMSE for Model 2 was 0.506 mm, and the RMSE for Model 3 was 0.135 mm.

To further evaluate the performance of the models, we plotted the experimental measurements of warpage deviation (flatness error on bottom face) of each scanned part against the predicted warpage deviation, and found the least-squares regression line. If the model predictions were equal to the measured data for each part, we would expect a slope equal to 1 and a y-intercept of 0. A plot was made for each of the models. Standardized residuals for the least-square regression line are plotted as well.

The results for Model 1 are shown in Fig. 7. The regression line has a slope of 0.13 and a y-intercept of 0.58. The coefficient of determination, R^2, is equal to 0.19, indicating that the model

did not accurately capture the observed behavior for all parts. The model predicts much more warping than was observed for the thinnest parts, with a height of 1.5 mm, which impacts the overall model fit significantly. (In Fig. 10, we found a best-fit line for each series of data points with the same thickness and printer separately, but we first wanted to evaluate the model performance at all datapoints simultaneously).

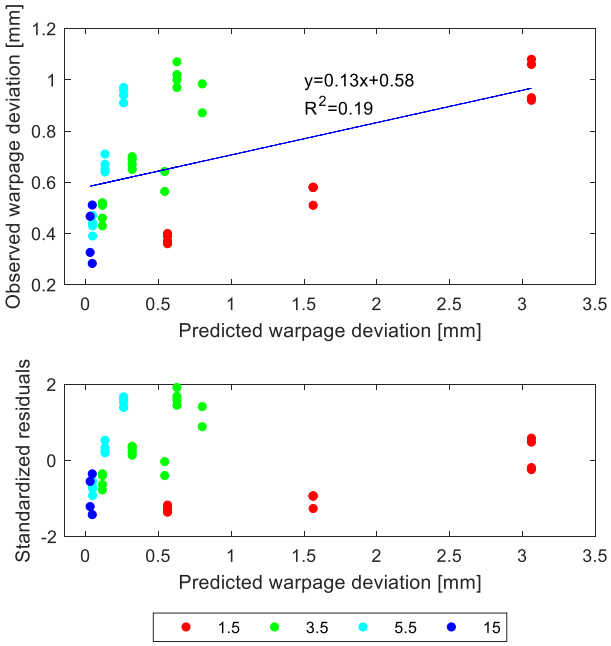

FIGURE 7: MODEL 1 HAD RELATIVELY POOR FIT FOR 1.5 MM PARTS. RESIDUALS TEND TO INCREASE LINEARLY WITH LENGTH FOR PARTS OF THE SAME HEIGHT. LEGEND INDICATES HEIGHT OF PARTS IN MM.

The results for Model 2 are shown in Fig. 8. Here, the model predicts warpage deviations much closer to the observed values for the 1.5 mm height parts, which improves the R^2, slope, and intercept values when compared with Model 1. However, there are still noticeable, distinct trends for series with varying heights.

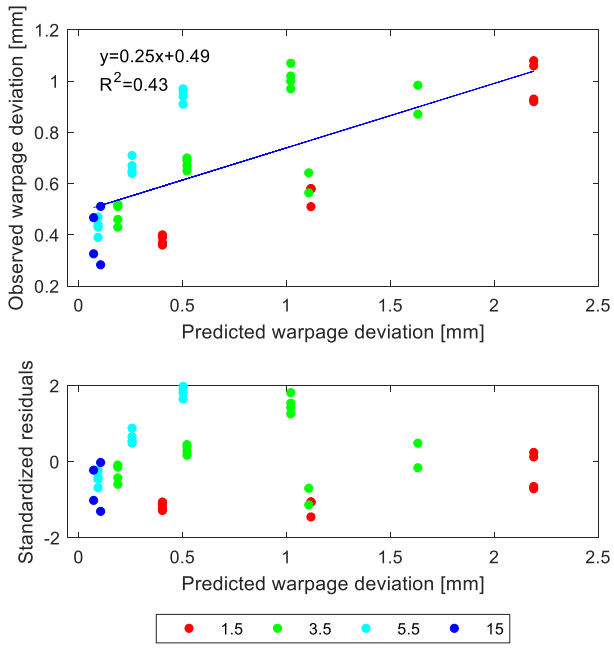

FIGURE 8: MODEL 2 PREDICTED DEVIATIONS MORE ACCURATELY FOR THE 1.5 MM PARTS BUT FIT IS STILL POOR AND PATTERNS IN THE RESIDUALS ARE STILL VISIBLE. LEGEND INDICATES HEIGHT OF PARTS IN MM.

Model 3, the empirical model, performed the best when applied to our entire dataset (Fig. 9). The slope and intercept are close to the ideal values of one and zero, respectively. However, this approach cannot resolve the small differences in warping due to differences in height. Another drawback to this approach is that the experimentally determined k value would need to be determined for each printer.

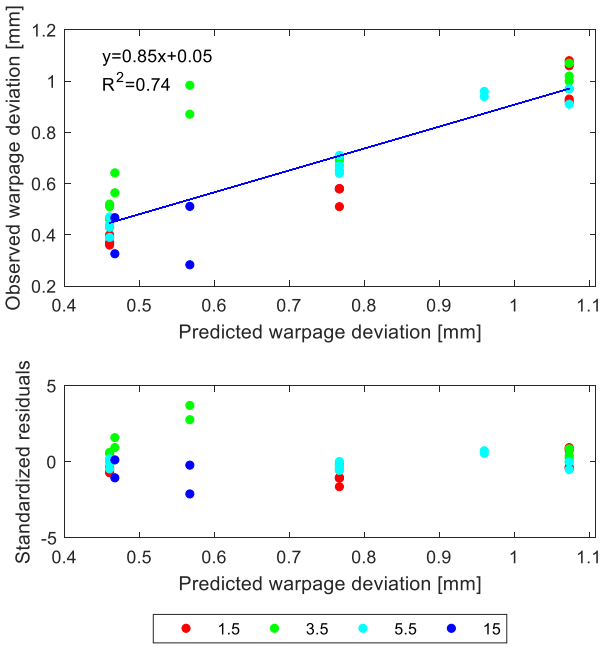

FIGURE 9: MODEL 3 HAD THE BEST FIT FOR ALL DATA, WITH NO NOTICABLE PATTERNS IN THE RESIDUALS. LEGEND INDICATES HEIGHT OF PARTS IN MM.

One interesting finding is that Model 1 and Model 2 both seemed to have too strong of a dependence on height. If height is held constant, there appears to be a more pronounced linear relationship between the observed and modeled warpage deviation. To explore this behavior further, we found a best-fit line for each series of data points with the same height and printer. For both Model 1 and Model 2, for a given printer and a fixed width, the observed and predicted data points generally fall along a line (Fig. 10 and Fig. 11, respectively). The parameters associated with each best-fit line are summarized in Table 6 for Model 1 and Table 7 for Model 2. Parts with a height of 15 mm were excluded because a line of best fit for that data would have resulted in a slope of nearly zero. It appears that the models did not capture the behavior of the 15 mm parts as well as they did for thinner parts, which may indicate that the models are most relevant for thin parts where part height is less than 15 mm.

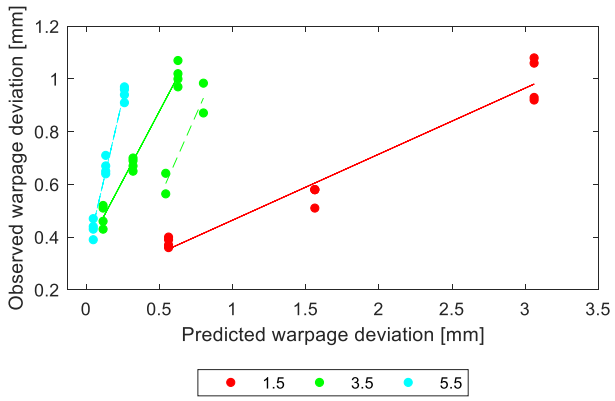

FIGURE 10: MODEL 1 PERFORMANCE WITH LINES OF BEST FIT FOR DIFFERENT COMINATIONS OF PART WIDTH AND PRINTER. DASHED AND SOLID LINES INDICATES PARTS PRINTED WITH THE LULZBOT AND DIMENSION, RESPECTIVELY.

TABLE 6: REGRESSION LINE PARAMETERS FOR WIDTHS TAKEN SEPARATELY FOR MODEL 1

Printer	Height [mm]	Intercept	Slope	R^2
Dimension	1.5	0.213	0.25	0.951
Dimension	3.5	0.325	1.05	0.976
LulzBot	3.5	-0.081	1.26	0.877
Dimension	5.5	0.330	2.38	0.978

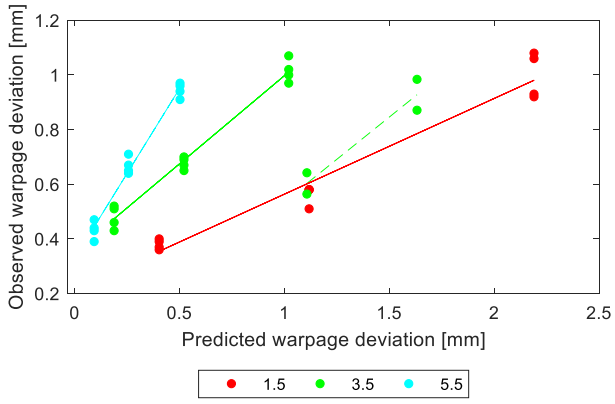

FIGURE 11: MODEL 2 PERFORMANCE WITH LINES OF BEST FIT FOR DIFFERENT COMINATIONS OF PART WIDTH AND PRINTER. DASHED AND SOLID LINES INDICATES PARTS PRINTED WITH THE LULZBOT AND DIMENSION, RESPECTIVELY.

TABLE 7: REGRESSION LINE PARAMETERS FOR WIDTHS TAKEN SEPARATELY FOR MODEL 2

Printer	Height [mm]	Intercept	Slope	R^2
Dimension	1.5	0.214	0.35	0.951
Dimension	3.5	0.352	0.64	0.976
LulzBot	3.5	-0.081	0.62	0.877
Dimension	5.5	0.323	1.24	0.978

For Models 1 and 2, the slope of the best-fit line increases as the part increases. These models are not capturing all of the physical behavior of the warping and how it is influenced by part height. Further study is needed to derive a more accurate analytical model that better captures the physical behavior.

An important consideration in evaluating the model performance is that the ultimate goal of this study was to find a model to estimate the risk of warping, not to predict the amount of warping deviation. All three models can predict the relative risk of warping for changes in length and width for a constant part height, and Models 1 and 2 both predicted that increasing height tended to decrease deviation, though the observed relationship was not as predicted. None of the three models could accurately predict relative risk of warping between different machines and materials (e.g., PLA versus ABS and LulzBot versus Dimension), at least for our measurement sample. However, there is promise that with improvements in how part height is considered in the models, the predictive accuracy of the models will increase. Even in their current state, all models captured the physical warping behavior to some extent and would likely be useful in providing preliminary design-for additive-manufacturing-feedback to designers who are exploring geometry or build orientation changes.

3.4 Future work

Below, we highlight four areas in need of further research:

1. Impact of adhesion and detachment of part during printing: From our height deviation measurements, it appeared that sharp corners resulted in larger curling at the corners than in filleted corners, possibly because the filleted corners had better adhesion to the build plate. We hypothesize that curling at sharp corners during printing may reduce internal stresses in the part, but this is an area in need of future research. Additionally, printing settings such as a raft or brim, adjusting build plate temperatures, and adding adhesives to the build plate can all can improve adhesion, which may reduce warping. A previous study found that using adhesive on build platform helped reduced deviations due to warping, even after the part was detached [8]. More research is needed to determine how these settings interact with part geometry and warping deviation.

2. Impact of toolpath and infill: It is currently unclear how part geometry interacts with the toolpath and infill percentage in determining the amount of warping deviation observed on a part. In the data we included here, two infill types were used: parts printed on the LulzBot used partial infill, while parts printed on the Dimension used a solid infill. This difference may explain some of the differences in the observed versus predicted trends for the two printers. Both printers deposited the infill at 45° angles, which has been cited as potentially increasing warping [17]. Raster angle and toolpath pattern are not included in the model, but these settings have been found to impact warping deviations in previous studies [14], [18], [23]. It may be possible to analytically model the impact of these settings on the part stiffness [24], but it may be more difficult to analytically model their impact on the temperature gradients in the part. More research is needed to determine the relative impact of geometry versus process settings like toolpath and infill.

3. Impact of more complex geometry: As a first step to exploring more complex geometry, we examined rectangular parts with varying height and with and without fillets. The geometry of the parts we tested can still be captured by width, height, and height, but these same parameters cannot capture more complicated geometry. In order to make effective DFAM tools based on the predictive models explored in this study, we need to be able to estimate this risk for a wide range of freeform part geometry that designers are interested in exploring. The analytical warping models we used here should be made more general for complex geometry, with geometry dependence represented using the cross-sectional area and second moment of area, rather than terms that are specific to rectangular geometry like length and width. Another area of future work is to expand the modeling capability for a wide range of part heights. The thickest part geometry we tested, 15 mm, seemed to be an outlier compared with the other, thinner geometries.

4. Filament material properties at printing conditions: The analytical models explored here make several simplifying assumptions regarding material behavior (e.g., Model 1 assumes that the FFF materials are linear-elastic and isotropic) but these assumptions are oversimplifications of the actual complex material behavior. There is anisotropy in the mechanical and thermomechanical behavior of AM parts [5]. We need to understand to what extent these assumptions and simplifications regarding material properties limit our predictive ability for the relative risk of warping. Another area of future research is to quantify the uncertainty regarding material properties for designers, and to help them understand how the uncertainty in properties impacts the ultimate uncertainty in the prediction of risk of warping.

5. Expanding research to more FFF printers: Here, we examined two FFF printers, the LulzBot TAZ 5 and the Dimension Elite. However, there are countless other common FFF machines currently in use, and the models we present here need to be validated for a wider range of these printers. If material properties for different filament types can be more fully constrained, it is likely that the predictive abilities of the analytical models will improve between different printers, but this area will need further experimentation.

4. CONCLUSION

This study identified that analytical and empirical models can estimate the warping deviation on parts printed using FFF to a certain extent. Existing models appear best suited for assessing the risk of warping rather than predicting the magnitude of warpage. Our findings suggest that better representation of the impact of part height could lead to improved predictions of warpage. Areas of future research include expanding our efforts into more complex geometry, other FFF printers, and further fundamental research on the role of adhesion and material properties in the warping process.

ACKNOWLEDGEMENTS

We thank the reviewers for their constructive feedback. This material is based upon work supported by the National Science Foundation Graduate Research Fellowship Program under Grant No. DGE-1752814. Any opinions, findings, and conclusions or recommendations expressed in this material are those of the author and do not necessarily reflect the views of the National Science Foundation.

REFERENCES

[1] M. K. Thompson *et al.*, "Design for Additive Manufacturing: Trends, opportunities, considerations, and constraints," *CIRP Ann. - Manuf. Technol.*, vol. 65, no. 2, pp. 737–760, 2016.

[2] T. Lieneke *et al.*, "Systematical determination of tolerances for additive manufacturing by measuring linear dimensions," in *Proceedings of the Solid Freeform Fabrication Symposium*, 2015, pp. 371–384.

[3] F. Bähr and E. Westkämper, "Correlations between Influencing Parameters and Quality Properties of Components Produced by Fused Deposition Modeling," *Procedia CIRP*, vol. 72, pp. 1214–1219, 2018.

[4] H. D. Budinoff, "Geometric Manufacturability Analysis for Additive Manufacturing," Doctoral Dissertation, Mechanical Engineering, University of California, Berkeley, 2019.

[5] B. N. Turner and S. A. Gold, "A review of melt extrusion additive manufacturing processes: II. Materials, dimensional accuracy, and surface roughness," *Rapid Prototyp. J.*, vol. 21, no. 3, pp. 250–261, 2015.

[6] M. Mahesh, Y. S. Wong, J. Y. H. Fuh, and H. T. Loh, "Benchmarking for comparative evaluation of RP systems and processes," *Rapid Prototyp. J.*, vol. 10, no. 2, pp. 123–135, 2004.

[7] C. Schmutzler, A. Zimmermann, and M. F. Zaeh, "Compensating warpage of 3D printed parts using free-form deformation," *Procedia CIRP*, vol. 41, pp. 1017–1022, 2016.

[8] M. S. Alsoufi and A. E. Elsayed, "Warping deformation of desktop 3D printed parts manufactured by open source fused deposition modeling (FDM) system," *Int. J. Mech. Mechatronics Eng.*, vol. 17, no. 4, pp. 7–16, 2017.

[9] Y. Zhang and K. Chou, "A parametric study of part distortions in fused deposition modelling using three-dimensional finite element analysis," *Proc. Inst. Mech. Eng. Part B J. Eng. Manuf.*, vol. 222, no. 8, pp. 959–967, 2008.

[10] Y. Zhang and Y. Chou, "Three-dimensional finite element analysis simulations of the fused deposition modelling process," *Proc. Inst. Mech. Eng. Part B J. Eng. Manuf.*, vol. 220, no. 10, pp. 1663–1671, 2006.

[11] A. Cattenone, S. Morganti, G. Alaimo, and F. Auricchio, "Finite Element Analysis of Additive Manufacturing Based on Fused Deposition Modeling: Distortions Prediction and Comparison With Experimental Data," *J. Manuf. Sci. Eng.*, vol. 141, no. 1, 2018.

[12] B. Courter, V. Savane, J. Bi, S. Dev, and C. J. Hansen, "Finite Element Simulation of the Fused Deposition Modelling Process," in *Proceedings of the NAFEMS World Congress*, June 2017.

[13] A. Armillotta, M. Bellotti, and M. Cavallaro, "Warpage of FDM parts: Experimental tests and analytic model," *Robot. Comput. Integr. Manuf.*, vol. 50, pp. 140–152, 2018.

[14] T. M. Wang, J. T. Xi, and Y. Jin, "A model research for prototype warp deformation in the FDM process," *Int. J. Adv. Manuf. Technol.*, vol. 33, pp. 1087–1096, 2007.

[15] P. Anhua, "Research on the Interlayer Stress and Warpage Deformation in FDM," in *2nd International Conference on Advanced Engineering Materials and Technology, AEMT*, 2012, pp. 1564–1567.

[16] A. Alafaghani, A. Qattawi, and M. A. Ablat, "Design Consideration for Additive Manufacturing: Fused Deposition Modelling," *Open J. Appl. Sci.*, vol. 7, pp. 291–318, 2017.

[17] J. Hämäläinen, "Semi-Crystalline Polyoefins in Fused Deposition Modeling," 2017.

[18] A. Guerrero-De-Mier, M. M. Espinosa, and M. Domínguez, "Bricking: A New Slicing Method to Reduce Warping," *Procedia Eng.*, vol. 132, pp. 126–131, 2015.

[19] J. W. Booth, J. Alperovich, P. Chawla, J. Ma, T. Reid, and K. Ramani, "The Design for Additive Manufacturing Worksheet," *J. Mech. Des.*, vol. 139, no. 10, 2017.

[20] Hexagon Metrology, "ROMER Absolute Arm Overview Brochure. Hexagon Metrology.," 2015. [Online]. Available: https://www.hexagonmi.com/~/media/Hexagon MI Legacy/hxrom/romer/general/brochures/ROMER Absolute Arm_overview_brochure_en.ashx.

[21] Ultimaker, "Technical Data Sheet PLA," 2018. [Online]. Available: https://ultimaker.com/download/74599/UM180821 TDS PLA RB V10.pdf.

[22] SD3D, "PLA Technical Data Sheet," 2017. [Online]. Available: https://www.sd3d.com/wp-content/uploads/2017/06/MaterialTDS-PLA_01.pdf.

[23] L. Xinhua, L. Shengpeng, L. Zhou, Z. Xianhua, C. Xiaohu, and W. Zhongbin, "An investigation on distortion of PLA thin-plate part in the FDM process," *Int. J. Adv. Manuf. Technol.*, vol. 79, no. 5–8, pp. 1117–1126, 2015.

[24] D. Croccolo, M. De Agostinis, and G. Olmi, "Experimental characterization and analytical modelling of the mechanical behaviour of fused deposition processed parts made of ABS-M30," *Comput. Mater. Sci.*, vol. 79, pp. 506–518, 2013.

